http://dx.doi.org/10.5012/bkcs.2013.34.11.3451

Fabrication and Characterization of Dodecyl-derivatized Silicon Nanowires for Preventing Aggregation

Donghee Shin and Honglae Sohn*

*Department of Chemistry, Chosun University, Gwangju 501-759, Korea. *E-mail: hsohn@chosun.ac.kr*
Received September 26, 2013, Accepted October 8, 2013

Single-crystalline silicon nanowires (SiNWs) were fabricated by using an electroless metal-assisted etching of bulk silicon wafers with silver nanoparticles obtained by wet electroless deposition. The etching of SiNWs is based on sequential treatment in aqueous solutions of silver nitrate followed by hydrofluoric acid and hydrogen peroxide. SEM observation shows that well-aligned nanowire arrays perpendicular to the surface of the Si substrate were produced. Free-standing SiNWs were then obtained using ultrasono-method in toluene. Alkyl-derivatized SiNWs were prepared to prevent the aggregation of SiNWs and obtained from the reaction of SiNWs and dodecene *via* hydrosilylation. Optical characterizations of SiNWs were achieved by FT-IR spectroscopy and indicated that the surface of SiNWs is terminated with hydrogen for fresh SiNWs and with dodecyl group for dodecyl-derivatized SiNWs, respectively. The main structures of dodecyl-derivatized SiNWs are wires and rods and their thicknesses of rods and wire are typically 150-250 and 10-20 nm, respectively. The morphology and chemical state of dodecyl-derivatized SiNWs are characterized by scanning electron microscopy, transmission electron microscopy, and X-ray photoelectron spectroscopy.

Key Words : Silicon nanowires, Hydrosilylation, Metal-assisted etching, Aggregation

Introduction

There is an enormous interest in the research and development of silicon nanomaterials for various applications in the fields of opto-electronics, photonics, photovoltaics,[1-4] field-effect transistors,[5-7] optical band pass filters, chemical and biological sensors, and drug delivery.[8-14] Due to material abundance and nontoxicity, the silicon-based materials are highly favored at a huge industrial infrastructure for low production/processing costs and high production yields. Bulk silicon does not emit visible light, because it is an indirect band gap material with a small exciton-binding energy (15 meV). However, low dimensional nanostructured-silicon materials such as quantum dots, nanocrystals, nanowires, and porous silicon have a direct band gap and emit visible light due to their quantum confinement effect. In recent years, many synthesis techniques for the silicon nanowires (SiNWs) have been developed.[15-20] Since silicon is a very important semiconductor material, Si NWs have attracted tremendous research interest due to their potential applications in the microelectronic industry. The fabrication of SiNWs can be achieved through the metal catalyzed growth, known as vapor-liquid-solid growth,[15] chemical vapor deposition or physical vapor deposition methods,[16] or electron beam evaporation.[17-20] These methods are quite accessible and well controlled. However, these techniques often require hazardous silicon precursors, high temperature, complex equipment, and other vigorous conditions. In addition, the growth of SiNWs is very slow and the coast is high.

In the recent years, electroless metal depositions (EMD) on a silicon substrate in ionic metal HF solution have been widely used in the microelectronic industries for preparing electrode, and patterning circuit board, and making ohmic contacts, because this technique has advantage such as simplicity, low operating temperature, and low cost.[21-24] Pt, Au, Pd, Cu, and Ni depositions on silicon wafers in HF solution have been extensively studied.[25] EMD is a localized micro-electrochemical redox reaction process in which both anodic and cathodic process occurs simultaneously at the silicon surface and involves the spontaneous oxidation of silicon atoms and the reduction of metal ions to metallic particles in the absence of an external source of electric current. The EMD technique has been extended to the fabrication of various nanostructures including SiNWs.[26,27] The morphologies of SiNWs can be affected by many factors such as the type, doping level, and orientation of the silicon wafer, concentration of H_2O_2 in the etchant, etching temperature, and etching time. However silicon-silicon bonds are easily oxidized[28] and a major drawback of SiNW dispersions is their thermodynamic driven tendency to lower their interfacial surface area with the environment and thus to aggregate. To prevent these issues, the hydrosilylation reaction of SiNWs could be an alternative method,[29] because the SiNWs are composed with Si-H surface. Therefore, it would be advantageous to store the SiNWs in a dry and stable state for their applications.

Herein, we reported the fabrication of free-standing SiNWs using ultrasono-method after simple chemical etching of silicon wafers in an aqueous HF solution containing silver nitrate at room temperature. Alkylation of SiNW based on hydrosilylation to prevent the aggregation and passivation of SiNWs was provided. This method allows the rapid fabrication of high-quality SiNWs dispersions.

Experimental Section

Preparation of SiNWs. Si <100> wafers (p-type, boron-doped, 500 μm thick), were used in this work. HF (49%), H_2O_2 (30%), H_2SO_4 (98%), NH_4OH (40%), 1-dodecene (> 99.0%) and $AgNO_3$ (> 99.9%) were purchased from Sigma–Aldrich. Silicon wafers were cut into 10 mm^2 pieces, which were washed in deionized water, acetone, and ethanol at room temperature to remove contaminated organics from the silicon surface. The wafer pieces were then cleaned in 50 mL oxidant solution containing H_2SO_4 and H_2O_2 (4:1) in a volume ratio 4:1 for 10 min under room temperature to form a thin oxide layer and then in 50 mL solution of NH_4OH/H_2O_2/H_2O (1:1:5) for 1 hour each. After each cleaning step, the wafer pieces were rinsed with excess deionized water. The cleaned silicon wafer pieces were then immersed in 50 mL cold 5% HF aqueous solution for 3 min under room temperature to give fresh H-terminated Si surfaces. The silicon wafers were immediately placed into 50 mL Ag coating solution containing 4.8 M HF and 0.04 M $AgNO_3$, which were slowly stirred for 1 min under ambient atmosphere. Ag particles were coated on silicon by immersing silicon pieces in that solution. After coating with a uniform layer of Ag nanoparticles (AgNPs), the silicon substrate was washed with water to remove extra Ag^+ ions and then immersed in oxidizing HF etching solution (50 mL) composed of 4.8 M HF and 30% H_2O_2 (10:1 v/v) in a reaction vessel. After 30 min etching in the dark under room temperature, the wafers were washed repeatedly with water and then immersed in dilute HNO_3 (1:1 v/v) to dissolve the Ag catalyst. The sample was rinsed with deionized water and dried at room temperature. The wafers were washed with 5% HF (10 mL) again to remove the oxide layer and then cleaned with water and dried under N_2 flow. For the isolation of free-standing SiNWs, the prepared SiNW array films were placed in 100 mL of toluene in a Schlenk flask under argon atmosphere, and then made into particles by ultrasonic fracture in toluene solution for 3 h. After the removal of all volatile liquids under a reduced pressure, SiNWs were stored in nitrogen atmosphere prior to use.

Hydrosilylation of SiNWs with Dodecene. 100 mg of SiNWs and platinum-cyclovinylmethylsiloxane catalyst (10 mg) were placed in a 50-mL Schlenk flask under an argon atmosphere. After 10-mL of 1-dodecene had been added, the reaction mixture was refluxed at 220 ^oC for 24 h. After the reaction, all removable liquids were evaporated under a reduced pressure to obtain the dodecyl-terminated SiNWs. Black powders as dodecyl-derivatized SiNWs were obtained and stored under argon atmosphere prior to use.

Instrumentation and Data Acquisition. FT-IR spectra were acquired with a Nicolet model 5700 FT-IR instrument in the diffuse reflectance mode (Spectra-Tech diffuse reflectance attachment) and absorption spectra were reported in absorbance units. Morphologies of dodecyl-derivatized SiNWs and as-prepared SiNW arrays were obtained by a cold field emission scanning electron microscopy (FE-SEM, S-4800, Hitachi). The high-resolution transmission electron microscopy (HR-TEM) employed in this work is a Philips TECNAI F20 microscope operating at 200 keV. The TEM specimen were prepared by dipping carbon micro-grids (Ted Pella Inc., 200 Mesh Copper Grid) into well-dispersed samples in NMP or ethanol. X-ray photoelectron spectroscopy (XPS) was performed in a conventional turbo-molecularly pumped UHV chamber with a MULTILAB 2000 System using monochromatic Mg Kα radiation (X-ray of 1253.6 eV) to analyze the composition and chemical states of products.

Results and Discussion

Silver particles were produced on the surface of silicon wafer using conventional EMD techniques. Figure 1(a) showed a SEM image of Ag-nanoparticle film deposited onto a p-type silicon wafer in HF/$AgNO_3$ for 1 min, indicating that the silver nanoparticles were evenly coated on the surface of silicon wafer and their sizes were in the range of 10 to 20 nm. The deposited silver nanoparticles form interconnected networks. After the electroless deposition of Ag-nanoparticles, the Ag-covered Si substrate was immersed in HF/H_2O_2 solution at room temperature. The etchant composition was 4.8 M HF and 30% H_2O_2 (10:1 v/v). Ag-coated silicon wafers were etched for 30 min in HF / H_2O_2 solution. Etching of silicon wafer proceeds very rapidly when silicon substrates covered with Ag-nanoparticles are immersed. The color of as-synthesized sample was black, indicating its excellent absorption capability. A high-quality, oriented, and H-terminated SiNW arrays were produced on silicon substrates under optimized etching conditions.

Figure 1(b) (top view) and 1(c) (side view) show that the initial stage of SiNW array formation on the silicon surface after 10 min etching. Silver nanoparticles start digging holes on the silicon substrate. After 30 min etching, Figure 1(d) shows SEM cross-sectional image of as-prepared SiNW array and displays a large-area aligned silicon nanowire array perpendicular to the silicon surface and the interface between SiNW array and the silicon substrate. The length of SiNW is about 50 microns and an etching rate of 1.7 μm/min is obtained with a metal assisted-etching in aqueous HF/H_2O_2 solution. Figure 1(e) shows SEM surface image of as-prepared SiNW array, indicating that SiNWs displayed a bundled structure due to the tendency to lower their interfacial surface area. The length of the SiNWs gradually increased with the increase of an etching time due to the sinking of silver nanoparticles into the bulk silicon. Figure 1(f) shows the sinking behavior of the Ag nanoparticles. The Ag nanoparticles are visible at the interface between SiNWs and the silicon substrate.

SiNWs were detached from the silicon substrate using ultrasono-method to create free-standing SiNWs and subjected to surface-derivatization with dodecene to prevent aggregation of SiNWs. Diffuse reflectance FT-IR spectroscopy was used to monitor the hydrosilylation reaction of SiNW samples. The FT-IR spectroscopy revealed that hydrosilylation using platinum catalyst exhibited the decrease of

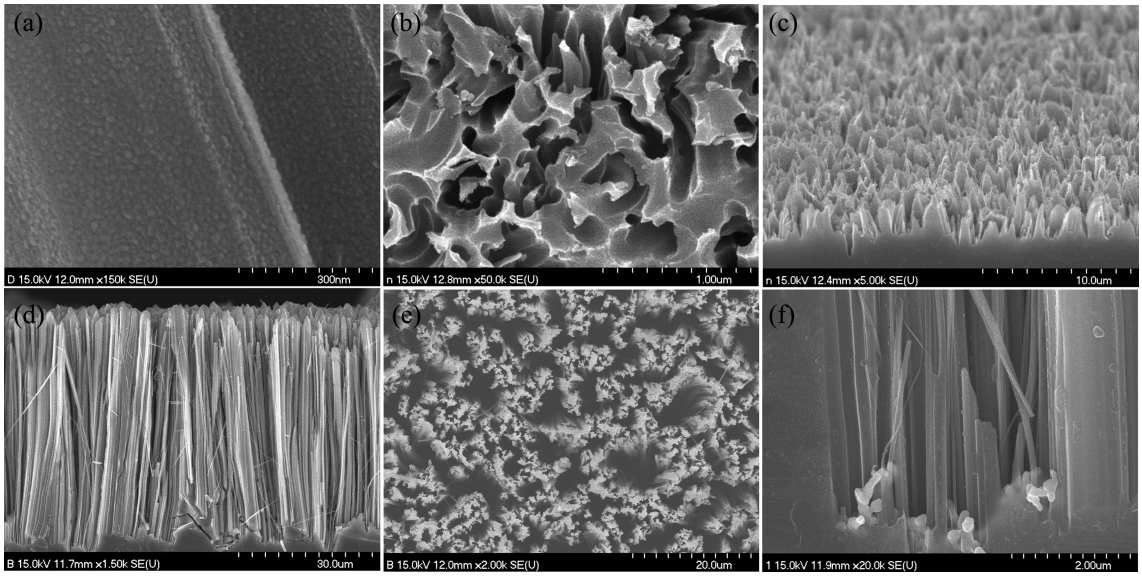

Figure 1. (a) SEM image of Ag-nanoparticle film deposited onto a p-type silicon surface in $HF/AgNO_3$ for 1 min. (b) SEM image of SiNW arrays prepared in 4.8 M HF containing 30% H_2O_2 for 10 min. (c) SEM cross-sectional image of the SiNW arrays shown in (B). (d) SEM cross-sectional image of the well-aligned SiNW arrays prepared for 30 min. (e) SEM side-view of well-aligned SiNW arrays shown in (D). (f) SEM image showing the sinking behavior of the Ag nanoparticles.

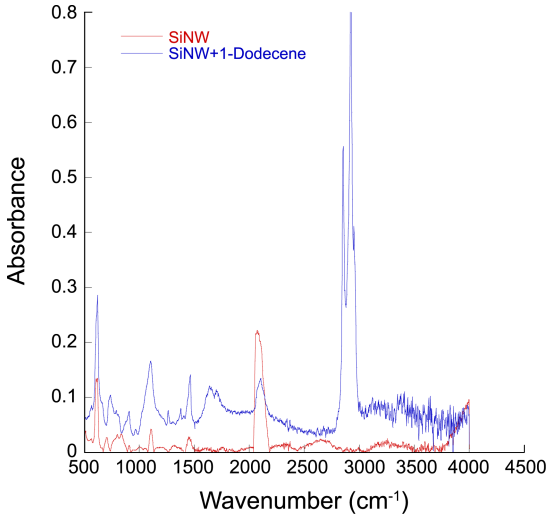

Figure 2. FT-IR spectra of free-standing SiNWs (bottom) and dodecyl-derivatized SiNWs (top).

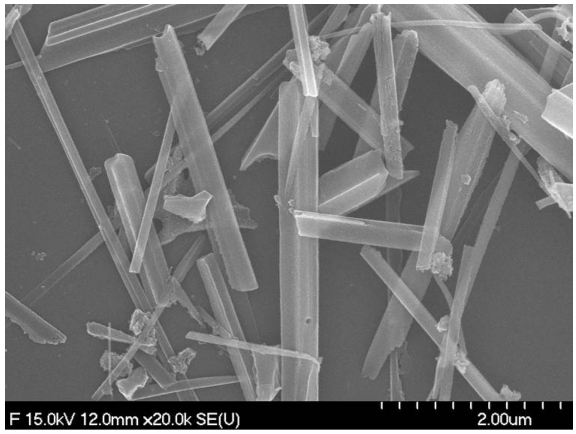

Figure 3. SEM image of dodecyl-derivatized SiNWs.

Si-H vibrational stretching frequency, indicating that the Si-H of SiNW reacted completely with the C=C moiety of dodecene. Figure 2 showed the FT-IR spectrum of as-prepared SiNWs and dodecyl-derivatized SiNWs. As-prepared SiNWs show a characteristic band centered at 2150 cm^{-1} for the ν(Si–H) stretching, indicating that the surface of SiNWs are terminated with hydrogen. After the surface modification of SiNWs with 1-dodecene *via* hydrosilylation, the FT-IR spectrum displayed additional bands characteristic of a strong aliphatic ν(C-H) stretching bands at 2858 and 2954 cm^{-1}. Surface derivatization led to a decrease of the Si-H vibrational band with very tiny Si-O-Si vibrational band at 1100 cm^{-1}. ν(OSi–H) vibratioal modes at 2277 cm^{-1} were not observed. Dodecyl-derivatized SiNWs were very stable in air against air-oxidation for several weeks and further oxidation did not proceed.

FE-SEM image in Figure 3 shows that dodecyl-derivatized SiNWs obtained from the hydrosilylation reaction of dodecene and SiNWs in the presence of platinum catalyst. The SEM image reveals that these silicon nanostructures have two main shapes such as wires and rods. Most of the silicon nanostructures are rods with typically 150-250 nm wide. The silicon nanostructures with diameters of 10-20 nm are thin wires. It is note that the surface of the silicon nanostructured-rods and wires are smooth and there is almost no diameter modulation along the length.

Figure 4 shows the HRTEM image of dodecyl-derivatized SiNWs. The methanol colloid was dried on a Cu TEM grid coated with a lacey carbon film and examined by HRTEM. The HRTEM image shows that the majority of SiNWs seen in the TEM are highly crystalline. The SiNWs are isolated

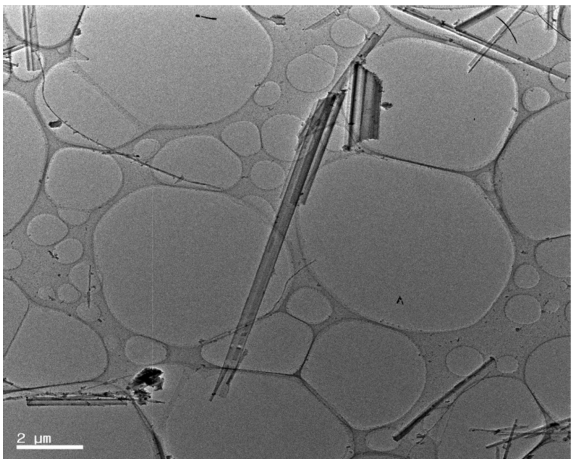

Figure 4. HRTEM image of dodecyl-derivatized SiNWs.

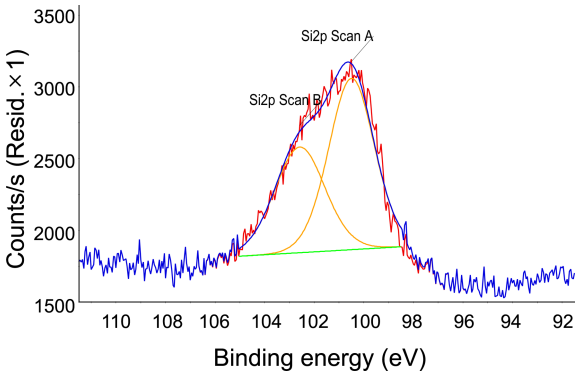

Figure 5. Si 2p XP spectrum of dodecyl-derivatized SiNWs.

from each other without significant overlap or agglomeration. The lattice plane imaged is typically Si [100]. The measured d spacings are 2.86 Å for [100]. The XPS spectrum of dodecyl-derivatized SiNWs shown in Figure 5 exhibited the characteristic Si 2p peak at E_B = 100.5 eV for the Si-C bonding and at E_B = 102.6 eV for the Si-O bonding. The latter peak is probably due to the surface oxidation of dodecyl-derivatized SiNWs during the treatment of samples. These assignments agree very well with previous XPS observations on air-exposed amorphous silicon carbide films on Si substrates.[30]

Conclusion

Si NWs array were successfully prepared by an electoless chemical etching of silicon wafer in etchant solution of HF and H_2O_2 for 30 min, after the deposition of the Ag-nanoparticle films using EMD. The etching of silicon wafer proceeds very rapidly and Si NWs array formed perpendicular to the silicon surface. The length of the SiNWs is about few microns and gradually increased with the increase of an etching time. The free-standing Si NWs were prepared using ultrasono-method. Surface-derivatization of SiNWs was achieved to prevent aggregation and oxidation of SiNWs. The morphology of SiNWs was obtained using FE-SEM. The main structures of SiNWs are wires and rods. The thicknesses of rods and wire are typically 150-250 nm and 10-20 nm, respectively. FT-IR spectrum showed a characteristic stretching vibration peaks for Si-H terminated SiNWs and aliphatic ν(C-H) stretching bands for dodecyl-terminated SiNWs, respectively. The HRTEM image shows that the majority of SiNWs seen in the TEM are highly crystalline. The XPS spectrum of dodecyl-derivatized SiNWs exhibits the characteristic Si 2p peak at EB = 100.5 eV for the Si-C bonding.

Acknowledgments. This research was supported (in part) research funds from Chosun University, 2013.

References

1. Hochbaum, A. I.; Fan, R.; He, R.; Yang, P. *Nano Lett.* **2005**, *5*, 457.
2. Schmidt, V.; Senz, S.; Gösele, U. *Nano Lett.* **2005**, *5*, 931.
3. Duan, X.; Huang, Y.; Cui, Y.; Wang, J.; Lieber, C. M. *Nature* **2001**, *409*, 66.
4. Kelzenberg, M. D.; Turner-Evans, D. B.; Kayes, B. M.; Filler, M. A.; Putnam, M. C.; Lewis, N. S.; Atwater, H. A. *Nano Lett.* **2008**, *8*, 710.
5. Koo, S.; Li, Q.; Edelstein, M. D.; Richter, C. A.; Vogel, E. M. *Nano Lett.* **2005**, *5*, 2519.
6. Cui, Y.; Zhong, Z. H.; Wang, D. L.; Wang, W. U.; Lieber, C. M. *Nano Lett.* **2003**, *3*, 149.
7. Duan, X. F.; Huang, Y.; Lieber, C. M. *Nano Lett.* **2002**, *2*, 487.
8. Koh, Y.; Park, J.; Kim, J.; Jang, S.; Woo, H.-G.; Sohn, H. *J. Nanosci. Nanotechnol.* **2010**, *10*, 3590.
9. Jang, S.; Kim, J.; Koh, Y.; Ko, Y. C.; Woo, H.-G.; Sohn, H. *J. Nanosci. Nanotechnol.* **2007**, *7*, 4049.
10. Jang, S.; Koh, Y.; Kim, J.; Park, J.; Park, C.; Kim, S. J.; Cho, S.; Ko, Y. C.; Sohn, H. *Mater. Lett.* **2008**, *62*, 552.
11. Park, C.; Kim, J.; Jang, S.; Woo, H.-G.; Ko, Y. C.; Sohn, H. *J. Nanosci. Nanotechnol.* **2010**, *10*, 3375.
12. Kim, J.; Jang, S.; Koh, Y.; Park, C.; Woo, H.-G.; Kim, S.; Sohn, H. *J. Nanosci. Nanotechnol.* **2008**, *8*, 4951.
13. Kim, S. G.; Kim, S.; Ko, Y. C.; Cho, S.; Sohn, H. *Colloids Surf. A: Physicochem. Eng. Aspects* **2008**, *313*, 398.
14. Koh, Y.; Jang, S.; Kim, J.; Kim, S.; Ko, Y. C.; Cho, S.; Sohn, H. *Colloids Surf. A: Physicochem. Eng. Aspects* **2008**, *313*, 328.
15. Wagner, R. S.; Ellis, W. C. *Appl. Phys. Lett.* **1964**, *4*, 89.
16. Wang, Y.; Schmidt, V.; Senz, S.; Gösele, U. *Nat. Nanotechnol.* **2006**, *1*, 186.
17. Sivakov, V.; Heyroth, F.; Falk, F.; Andrä, G.; Christiansen, S. H. *J. Cryst. Growth* **2007**, *300*, 288.
18. Sivakov, V.; Andrä, G.; Himcinschi, C.; Gösele, U.; Zahn, D. R. T.; Christiansen, S. *Appl. Phys. A: Mater. Sci. Process* **2006**, *85*, 311.
19. Fuhrmann, B.; Leipner, H. S.; Höche, H.-R.; Schubert, L.; Werner, P.; Gösele, U. *Nano Lett.* **2005**, *5*, 2524.
20. Oh, S. H.; van Benthem, K.; Molina, S. I.; Borisevich, A. Y.; Luo, W.; Werner, P.; Zakharov, N. D.; Kumar, D.; Pantelides, S. T.; Pennycook, S. J. *Nano Lett.* **2008**, *8*, 1016.
21. Kawashima, T.; Mizutani, T.; Nakagawa, T.; Torii, H.; Saitoh, T.; Komori, K.; Fujii, M. *Nano Lett.* **2008**, *8*, 362.
22. Gorostiza, P.; Kulandainathan, M. A.; Diaz, R.; Sanz, F.; Allongue, P.; Morante, J. R. *J. Electrochem. Soc.* **2000**, *147*, 1026.
23. Porter, L. A.; Choi, H. C.; Ribbe, A. E.; Buriak, J. M. *Nano Lett.* **2002**, *2*, 1067.
24. Magagnin, L.; Maboudian, R.; Carraro, C.; *J. Phys. Chem. B* **2002**, *106*, 401.
25. Peng, K.-Q.; Yan, Y.-J.; Gao, S.-P.; Zhu, J. *Adv. Mater.* **2002**, *14*, 1164.

26. Peng, K.; Hu, J.; Yan, Y.; Wu, Y.; Fang, H.; Xu, Y.; Lee, S. T.; Zhu, J. *Adv. Funct. Mater.* **2006**, *16*, 387.
27. Peng, K.; Xu, Y.; Wu, Y.; Yan, Y.; Lee, S.-T.; Zhu, J. *Small* **2005**, *1*, 1062.
28. Sohn, H.; Tan, R. P.; Powell, D. R.; West, R. *Organometallics* **1994**, *13*, 1390.
29. Cho, E. J.; Lee, V.; Yoo, B. R.; Jung, I. N.; Sohn, H.; Powell, D. R.; West, R. *Organometallics* **1997**, *16*, 4200.
30. Kennou, S.; Ladas, S.; Paloura, E. C.; Kalomiros, J. A. *Appl. Surf. Sci.* **1995**, *90*, 283.